

Detector-Independent Verification of Quantum Light

J. Sperling,^{1,*} W. R. Clements,¹ A. Eckstein,¹ M. Moore,¹ J. J. Renema,¹ W. S. Kolthammer,¹
S. W. Nam,² A. Lita,² T. Gerrits,² W. Vogel,³ G. S. Agarwal,⁴ and I. A. Walmsley¹

¹*Clarendon Laboratory, University of Oxford, Parks Road, Oxford OX1 3PU, United Kingdom*

²*National Institute of Standards and Technology, 325 Broadway, Boulder, Colorado 80305, USA*

³*Institut für Physik, Universität Rostock, Albert-Einstein-Straße 23, D-18059 Rostock, Germany*

⁴*Texas A&M University, College Station, Texas 77845, USA*

(Dated: August 30, 2021)

We introduce a method for the verification of nonclassical light which is independent of the complex interaction between the generated light and the material of the detectors. This is accomplished by means of a multiplexing arrangement. Its theoretical description yields that the coincidence statistics of this measurement layout is a mixture of multinomial distributions for any classical light field and any type of detector. This allows us to formulate bounds on the statistical properties of classical states. We apply our directly accessible method to heralded multiphoton states which are detected with a single multiplexing step only and two detectors, which are in our work superconducting transition-edge sensors. The nonclassicality of the generated light is verified and characterized through the violation of the classical bounds without the need for characterizing the used detectors.

Introduction.— The generation and verification of nonclassical light is one of the main challenges for realizing optical quantum communication and computation [1–4]. Therefore, robust and easily applicable methods are required to detect quantum features for real-world applications; see, e.g., [5, 6].

The complexity of producing reliable sensors stems from the problem that new detectors need to be characterized. For this task, various techniques, such as detector tomography [7–12], have been developed. However, such a calibration requires many resources, for example, computational or numerical analysis, reference measurements, etc. From such complex procedures, the interaction between quantum light and the bulk material of the detector can be inferred and quantum features can be uncovered. Nevertheless, the verification of nonclassicality also depends on the bare existence of criteria that are applicable to this measurement. Here, we prove that detectors with a general response to incident light can be employed in an optical detection scheme, which is well characterized, to identify nonclassical radiation fields based on simple nonclassicality conditions.

The concept of device independence has recently gained a lot of attention because it allows one to employ even untrusted devices; see, e.g., [13]. For instance, device-independent entanglement witnesses can be used without relying on properties of the measurement system [14, 15]. It has been further studied to perform communication and computation tasks [16, 17]. Detector independence has been also applied to state estimation and quantum metrology [18, 19] to gain knowledge about a physical system which might be too complex for a full characterization.

In parallel, remarkable progress has been made in the field of well-characterized photon-number-resolving (PNR) detectors [20, 21]. A charge-coupled-device camera is one example of a system that can record many

photons at a time. However, it also suffers inherent read-out noise. Still, the correlation between different pixels can be used to infer quantum correlated light [22–24]. Another example of a PNR device is a superconducting transition-edge sensor (TES) [25–27]. This detector requires a cryogenic environment, and its operation is based on superconductivity. Hence, a model for this detector would require the quantum mechanical treatment of a solid-state bulk material which interacts with a quantized radiation field in the frame of low-temperature physics.

Along with the development of PNR detectors, multiplexing layouts define another approach to realize photon-number resolution [28–33]. The main idea is that an incident light field, which consists of many photons, is split into a number of spatial or temporal modes, which consist of a few photons only. These resulting beams are measured with single-photon detectors which do not have any photon-number-resolution capacity. They can only discriminate between the presence (“click”) and absence of absorbed photons. Hence, the multiplexing is used to get some insight into the photon statistics despite the limited capacity of the individual detectors. With its resulting binomial click-counting statistics, one can verify nonclassical properties of correlated light fields [34–38]. Recently, a multiplexing layout has been used in combination with TESs to characterize quantum light with a mean photon number of 50 and a maximum number of 80 photons for each of the two correlated modes [39].

In this Letter, we formulate a method to verify nonclassical light with arbitrary detectors. This technique is based on a well-defined multiplexing scheme and individual detectors which can discriminate different measurement outcomes. The resulting correlation measurement is always described as a mixture of multinomial distributions in classical optics. Based on this finding, we formulate nonclassicality conditions in terms of covariances to directly certify nonclassical light. Nonclassical light

is defined in this work as a radiation field which cannot be described as a statistical mixture of coherent light [40, 41]. We demonstrate our approach by producing heralded photon-number states from a parametric down-conversion (PDC) source. Already a single multiplexing step is sufficient to verify the nonclassicality of such states without the need to characterize the used TESs. In addition to our method presented here, a complementary study is provided in Ref. [42]. There we use a quantum-optical framework to perform additional analysis of the measurement layout under study.

Theory.— The detection scenario is shown in Fig. 1. Its robustness to the detector response is achieved by the multiplexing layout whose optical elements, e.g., beam splitters, are much simpler and better characterized than the detectors. Our only broad requirement is that the measured statistics of the detectors are relatively similar to each other. Here we are not using multiplexing to improve the photon-number detection (see, e.g., Ref. [39]). Rather, we employ this scheme to get nonclassicality criteria that are independent of the properties of the individual detectors.

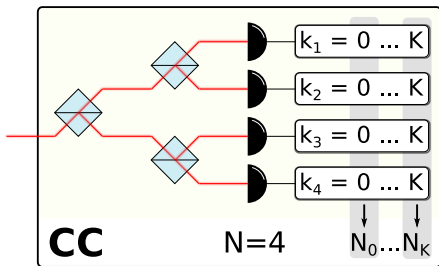


FIG. 1. (Color online) Multiplexed click-counting (CC) layout consisting of $N = 4$ individual detectors. Incident light is split into N beams with similar intensities. Each of the N detectors returns a measurement outcome k_n . The number of detectors N_k with the same outcome $0 \leq k \leq K$ is recorded.

First, we consider a single coherent, classical light field. The detector can resolve arbitrary outcomes $k = 0, \dots, K$ —or, equivalently, $K + 1$ bins [43]—which have a probability p_k . If the light is split by 50/50 beam splitters as depicted in Fig. 1 and measured with N individual and identical detectors, we get the probability $p_{k_1} \dots p_{k_N}$ to measure k_1 with the first detector, k_2 with the second detector, etc. Now, N_k is defined as the number of individual detectors which measure the same outcome k . This means we have N_0 times the outcome 0 together with N_1 times the outcome 1, etc., from the N detectors, $N = N_0 + \dots + N_K$. For example, $k_1 = K$ and $k_2 = k_3 = k_4 = 0$ yields $N_K = 1$ and $N_0 = 3$ for $N = 4$ detectors ($N_k = 0$ for all $0 < k < K$). The probability to get any given combination of outcomes, N_0, \dots, N_K , from the probabilities $p_{k_1} \dots p_{k_N}$ is known to follow a

multinomial distribution [44],

$$c(N_0, \dots, N_K) = \frac{N!}{N_0! \dots N_K!} p_0^{N_0} \dots p_K^{N_K}. \quad (1)$$

To ensure a general applicability, we counter any deviation from the 50/50 splitting and differences of the individual detectors by determining a corresponding systematic error (in our experiment in the order of 1%), see the Supplemental Material [45] for the error analysis.

For a different intensity, the probabilities p_k of the individual outcomes k might change. Hence, we consider in the second step a statistical mixture of arbitrary intensities. This generalizes the distribution in Eq. (1) by averaging over a classical probability distribution P ,

$$c(N_0, \dots, N_K) = \left\langle \frac{N!}{N_0! \dots N_K!} p_0^{N_0} \dots p_K^{N_K} \right\rangle \\ = \int dP(p_0, \dots, p_K) \frac{N!}{N_0! \dots N_K!} p_0^{N_0} \dots p_K^{N_K}. \quad (2)$$

Because any light field in classical optics can be considered as an ensemble of coherent fields [40, 41], the measured statistics of the setup in Fig. 1 follows a mixture of multinomial distributions (2). This is not necessarily true for nonclassical light as we will demonstrate. The distribution (2) applies to arbitrary detectors and includes the case of on-off detectors ($K = 1$), which yields a binomial distribution [46]. Also, we determine the number of outcomes, $K + 1$, directly from our data.

Let us now formulate a criterion that allows for the identification of quantum correlations. The mean values of multinomial statistics obey $\overline{N_k} = N p_k$ [44]. Averaging over P yields

$$\overline{N_k} = N \langle p_k \rangle. \quad (3)$$

In the same way, we get for the second-order moments, $\overline{N_k N_{k'}} = N(N-1)p_k p_{k'} + \delta_{k,k'} N p_k$ [44] with $\delta_{k,k'} = 1$ for $k = k'$ and $\delta_{k,k'} = 0$ otherwise, an averaged expression

$$\overline{N_k N_{k'}} = N(N-1) \langle p_k p_{k'} \rangle + \delta_{k,k'} N \langle p_k \rangle. \quad (4)$$

Thus, we find the covariance from Eqs. (3) and (4),

$$\overline{\Delta N_k \Delta N_{k'}} = N \langle p_k \rangle (\delta_{k,k'} - \langle p_{k'} \rangle) \\ + N(N-1) \langle \Delta p_k \Delta p_{k'} \rangle. \quad (5)$$

Note that the multinomial distribution has the covariances $\overline{\Delta N_k \Delta N_{k'}} = N p_k (\delta_{k,k'} - p_{k'})$ [44]. Multiplying Eq. (5) with N and using Eq. (3), we can introduce the $(K + 1) \times (K + 1)$ matrix

$$M = \left(N \overline{\Delta N_k \Delta N_{k'}} - \overline{N_k} (N \delta_{k,k'} - \overline{N_{k'}}) \right)_{k,k'=0,\dots,K} \\ = N^2 (N-1) \langle \langle \Delta p_k \Delta p_{k'} \rangle \rangle_{k,k'=0,\dots,K}. \quad (6)$$

As the covariance matrix $(\langle \Delta p_k \Delta p_{k'} \rangle)_{k,k'}$ is nonnegative for any classical probability distribution P , we can conclude: We have a nonclassical light field if

$$0 \not\leq (N \overline{\Delta N_k \Delta N_{k'}} - \overline{N_k} \overline{N_{k'}})_{k,k'=0,\dots,K}; \quad (7)$$

i.e., the symmetric matrix M in Eq. (6) has at least one negative eigenvalue. In other words, $M \not\geq 0$ means that fluctuations of the parameters p_k in $(\langle \Delta p_k \Delta p_{k'} \rangle)_{k,k'}$ are below the classical threshold of zero. Based on condition (7), we will experimentally certify nonclassicality.

Experimental setup.— Our experimental implementation is shown in Fig. 2(a). A PDC source produces correlated photons. Conditioned on the detection of k clicks from the heralding detector, we measure the click-counting statistics $c(N_0, \dots, N_K)$, Eq. (2). The key components of our experiment are (i) the PDC source and (ii) the three TESs used as our heralding detector and as our two individual detectors after the multiplexing step.

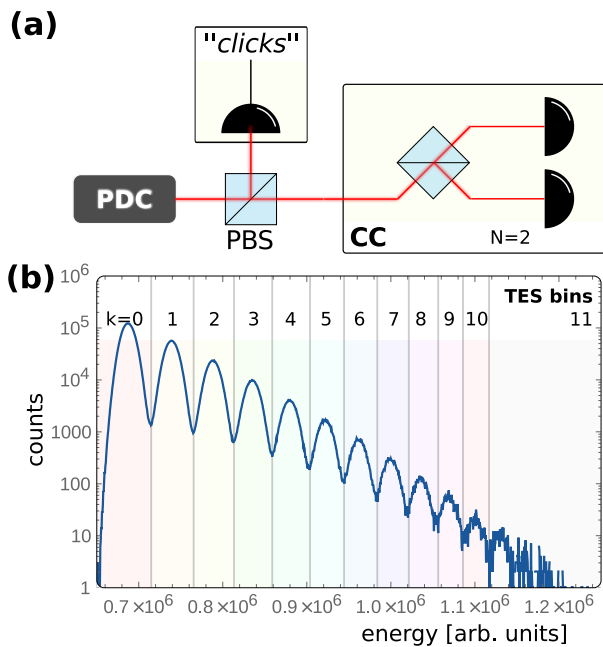


FIG. 2. (Color online) Panel (a) depicts the experimental arrangement. A PDC source produces correlated photon pairs which are separated with a polarizing beam splitter (PBS). A conditioning to a certain outcome (labeled as “click”) of a single TES yields a certain number of photons in the other beam. The latter signal is measured with a multiplexing scheme that consists of $N = 2$ TESs [cf. Fig. 1]. Panel (b) shows the binning into $K + 1$ possible outcomes (bins). The energies that are counted with a TES (shown for the heralding detector) can be separated into 12 bins.

(i) PDC source. Our PDC source is a waveguide-written 8 mm-long periodically poled potassium titanyl phosphate crystal. We pump a type-II spontaneous PDC process with laser pulses at 775 nm and a full width at half maximum of 2 nm at a repetition rate of 75 kHz. The heralding idler mode (horizontal polarization) is centered

at 1554 nm, while the signal mode (vertical polarization) is centered at 1546 nm. The output signal and idler pulses are spatially separated with a PBS. The pump beam is discarded using an edge filter. Subsequently, the other beams are filtered by 3 nm bandpass filters in order to filter out the broadband background which is typically generated in dielectric nonlinear waveguides [47].

(ii) TES detectors. We use superconducting TESs [25] as our detectors. They consist of $25 \mu\text{m} \times 25 \mu\text{m} \times 20 \text{nm}$ slabs of tungsten inside an optical cavity designed to maximize absorption at 1500 nm. They are maintained at their transition temperature by Joule heating caused by a voltage bias, which is self-stabilized via an electrothermal feedback effect [48]. When photons are absorbed, the increase in temperature causes a corresponding electrical signal which is picked up and amplified by a superconducting quantum interference device (SQUID) module and amplified at room temperature. This results in complex time-varying signals of about $5 \mu\text{s}$ duration. Our TESs are operated within a dilution refrigerator with a base temperature of about 70 mK. The estimated detection efficiency is $0.98^{+0.02}_{-0.08}$ [49]. The electrical throughput is measured using a waveform digitizer and assigns a bin (described below) to each output pulse [50]. We process incoming signals at a speed of up to 100 kHz.

The time integral of the measured signal results in an energy whose counts are shown in Fig. 2(b) for the heralding TES. It also indicates a complex, nonlinear response of the TESs [45]. The energies are binned into $K + 1$ different intervals. One typically fits those counts with a number of functions or histograms to get the photon statistics via numerical reconstruction algorithms for the particular detector. Our bins—also the number of them—are solely determined from the measured data by simply dividing our recorded signal into disjoint energy intervals [Fig. 2(b)]. This does not require any detector model or reconstruction algorithms. Above a threshold energy, no further peaks can be significantly resolved and those events are collected in the last bin. No measured event is discarded. Our heralding TES allows for a resolution of $K + 1 = 12$ outcomes. Because of the splitting of the photons on the beam splitter in the multiplexing step, the data from the other two TESs yield a reduced distinction between $K + 1 = 8$ outcomes.

Results.— Condition (7) can be directly applied to the measured statistics $c(N_0, \dots, N_K)$ by sampling mean values, variances, and covariances [Eq. (6)]. In Fig. 3, we show the resulting nonclassicality of the heralded states. As the minimal eigenvalue of M has to be non-negative for classical light, this eigenvalue is depicted in Fig. 3.

To discuss our results, we compare our findings with a simple, idealized model. Our produced PDC state can be approximated by a two-mode squeezed-vacuum state which has a correlated photon statistics, $p(n, n') = (1 - \lambda) \lambda^n \delta_{n,n'}$, where $n(n')$ is the signal(idler) photon number and $r \geq 0$ ($\lambda = \tanh^2 r$) is the squeezing parameter which

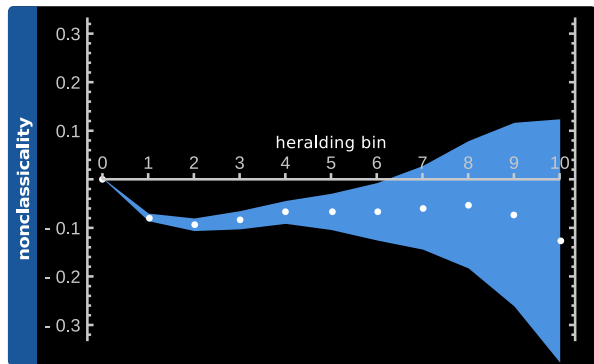


FIG. 3. (Color online) The minimal eigenvalue of the matrix M in Eq. (6) is shown including its error bars (shaded area) [45] as a function of the generated states, which are defined by the bin of the heralding TES. A negative value is inconsistent with classical optics and, therefore, verifies nonclassical light.

is a function of the pump power of the PDC process [51]. Heralding with an ideal PNR detector, which can resolve any photon number with a finite efficiency $\tilde{\eta}$, we get a conditioned statistics of the form

$$p(n|k) = \mathcal{N}_k \binom{n}{k} \tilde{\eta}^k (1 - \tilde{\eta})^{n-k} (1 - \lambda) \lambda^n, \quad (8)$$

$$\text{with } \mathcal{N}_k = \frac{(1 - \lambda)(\lambda \tilde{\eta})^k}{[1 - \lambda(1 - \tilde{\eta})]^{k+1}},$$

for the k th heralded state and $p(n|k) = 0$ for $n < k$ and $\lambda^0 = 1$. Here \mathcal{N}_k is a normalization constant as well as the probability that the k th state is realized. The signal includes at least $n \geq k$ photons if k photoelectric counts have been recorded by the heralding detector.

In the ideal case, the heralding to the 0th bin yields a thermal state [Eq. (8)] and in the limit of vanishing squeezing a vacuum state, $p(n|0) = \delta_{n,0}$ for $\lambda \rightarrow 0$. Hence, we expect that the measured statistics is close to a multinomial, which implies $M \approx 0$. Our data are consistent with this consideration, cf. Fig. 3.

Using an ideal detector, a heralding to higher bin numbers would give a nonclassical Fock state with the corresponding photon number. The nonclassical character of the experimentally realized multiphoton states is certified in Fig. 3. The generation of k photon pairs in the PDC is less likely for higher photon numbers, $\mathcal{N}_k \propto \lambda^k$. Hence, this reduced count rate of events results in the increasing contribution of the statistical error in Fig. 3. The highest significance of nonclassicality is found for lower heralding bins.

Furthermore, we studied our criterion (7) as a function of the pump power in Fig. 4 to demonstrate its impact on the nonclassicality. The conditioning to zero clicks of the heralding TES is consistent with a classical signal. For higher heralding bins, we observe that the nonclassicality is larger for decreasing pump powers as the distribution in Eq. (8) becomes closer to a pure Fock state. We

can also observe in Fig. 4 that the error is larger for smaller pump powers as fewer photon pairs are generated ($\mathcal{N}_k \propto \lambda^k$).

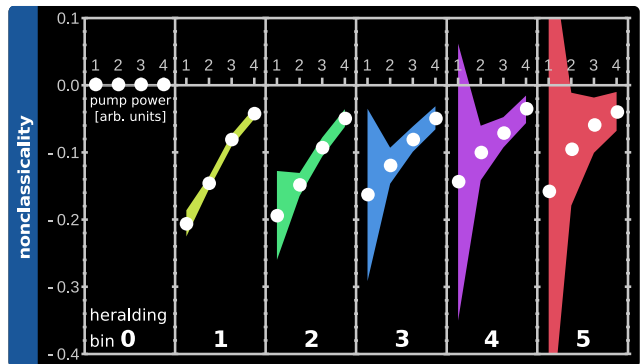


FIG. 4. (Color online) The minimal eigenvalue of M of the first six heralded states is shown as a function of the pump power. The nonclassicality (negative values) decreases with increasing power. However, the verification is more significant for higher pump powers.

Note that the nonclassicality is expressed in terms of the photon-number correlations. If our detector would allow for a phase resolution, we could observe the increase of squeezing with increasing pump power. This suggests a future enhancement of the current setup. Moreover, an implementation of multiple multiplexing steps ($N > 2$) would allow one to measure higher-order moments [42], which renders it possible to certify nonclassicality beyond second-order moments [36, 52, 53].

Conclusions.— We have formulated and implemented a robust and easily accessible method that can be applied to verify nonclassical light with arbitrary detectors. Based on a multiplexing layout, we showed that a mixture of multinomial distributions describes the measured statistics in classical optics independently of the specific properties of the individual detectors. We derived classical bounds on the covariance matrix whose violation is a clear signature of nonclassical light. We applied our theory to an experiment consisting of a single multiplexing step and two superconducting transition-edge sensors. We successfully demonstrated the nonclassicality of heralded multiphoton states. We also studied the dependence on the pump power of our spontaneous parametric-down-conversion light source.

Our method is a straightforward technique that also applies to, e.g., temporal multiplexing or other types of individual detectors, e.g., multipixel cameras. It also includes the approach for avalanche photodiodes [34, 35] in the special case of a binary outcome. Because our theory applies to general detectors, one challenge was to apply it to superconducting transition-edge sensors whose characteristics are less well understood than those of commercially available detectors. Our nonclassicality analysis is only based on covariances between different outcomes

which requires neither sophisticated data processing nor a lot of computational time. Hence, it presents a simple and yet reliable tool for characterizing nonclassical light for applications in quantum technologies.

Acknowledgements. — The project leading to this application has received funding from the European Union’s Horizon 2020 research and innovation programme under grant agreement No. 665148 (QCUMbER). A. E. is supported by EPSRC EP/K034480/1. J. J. R. is supported by the Netherlands Organization for Scientific Research (NWO). W. S. K. is supported by EPSRC EP/M013243/1. S. W. N., A. L., and T. G. are supported by the Quantum Information Science Initiative (QISI). I. A. W. acknowledges an ERC Advanced Grant (MOQUACINO). The authors thank Johan Fopma for technical support. The authors gratefully acknowledge helpful comments by Tim Bartley and Omar Magaña-Loaiza.

Note. — This work includes contributions of the National Institute of Standards and Technology, which are not subject to U.S. copyright.

* jan.sperling@physics.ox.ac.uk

- [1] E. Knill, R. Laflamme, and G. J. Milburn, A scheme for efficient quantum computation with linear optics, *Nature (London)* **409**, 46 (2001).
- [2] P. Kok, W. J. Munro, K. Nemoto, T. C. Ralph, J. P. Dowling, and G. J. Milburn, Linear optical quantum computing with photonic qubits, *Rev. Mod. Phys.* **79**, 135 (2007).
- [3] N. Gisin and R. Thew, Quantum communication, *Nat. Photon.* **1**, 165 (2007).
- [4] J. H. Shapiro, The Quantum Theory of Optical Communications, *IEEE J. Sel. Top. Quantum Electron.* **15**, 1547 (2009).
- [5] N. Thomas-Peter, B. J. Smith, A. Datta, L. Zhang, U. Dorner, and I. A. Walmsley, Real-World Quantum Sensors: Evaluating Resources for Precision Measurement, *Phys. Rev. Lett.* **107**, 113603 (2011).
- [6] F. E. Becerra, J. Fan, and A. Migdall, Photon number resolution enables quantum receiver for realistic coherent optical communications, *Nat. Photon.* **9**, 48 (2015).
- [7] A. Luis and L. L. Sánchez-Soto, Complete Characterization of Arbitrary Quantum Measurement Processes, *Phys. Rev. Lett.* **83**, 3573 (1999).
- [8] G. M. D’Ariano, L. Maccone, and P. Lo Presti, Quantum Calibration of Measurement Instrumentation, *Phys. Rev. Lett.* **93**, 250407 (2004).
- [9] M. Lobino, D. Korystov, C. Kupchak, E. Figueroa, B. C. Sanders, and A. I. Lvovsky, Complete characterization of quantum-optical processes, *Science* **322**, 563 (2008).
- [10] J. S. Lundeen, A. Feito, H. Coldenstrodt-Ronge, K. L. Pregnell, C. Silberhorn, T. C. Ralph, J. Eisert, M. B. Plenio, and I. A. Walmsley, Tomography of quantum detectors, *Nat. Phys.* **5**, 27 (2009).
- [11] L. Zhang, A. Datta, H. B. Coldenstrodt-Ronge, X.-M. Jin, J. Eisert, M. B. Plenio, and I. A. Walmsley, Recursive quantum detector tomography, *New J. Phys.* **14**, 115005 (2012).
- [12] G. Brida, L. Ciavarella, I. P. Degiovanni, M. Genovese, A. Migdall, M. G. Mingolla, M. G. A. Paris, F. Piacentini, and S. V. Polyakov, Ancilla-Assisted Calibration of a Measuring Apparatus, *Phys. Rev. Lett.* **108**, 253601 (2012).
- [13] J. Kaniewski and S. Wehner, Device-independent two-party cryptography secure against sequential attacks, *New J. Phys.* **18**, 055004 (2016).
- [14] C. Branciard, D. Rosset, Y.-C. Liang, and N. Gisin, Measurement-Device-Independent Entanglement Witnesses for All Entangled Quantum States, *Phys. Rev. Lett.* **110**, 060405 (2013).
- [15] Q. Zhao, X. Yuan, and X. Ma, Efficient measurement-device-independent detection of multipartite entanglement structure, *Phys. Rev. A* **94**, 012343 (2016).
- [16] C. C. W. Lim, B. Korzh, A. Martin, F. Bussières, R. Thew, and H. Zbinden, Detector-Device-Independent Quantum Key Distribution, *Appl. Phys. Lett.* **105**, 221112 (2014).
- [17] A. Gheorghiu, E. Kashefi, and P. Walde, Robustness and device independence of verifiable blind quantum computing, *New J. Phys.* **17**, 083040 (2015).
- [18] M. Cooper, M. Karpinski, and B. J. Smith, Quantum state estimation with unknown measurements, *Nat. Commun.* **5**, 4332 (2014).
- [19] M. Altorio, M. G. Genoni, F. Somma, and M. Barbieri, Metrology with Unknown Detectors, *Phys. Rev. Lett.* **116**, 100802 (2016).
- [20] C. Silberhorn, Detecting quantum light, *Contemp. Phys.* **48**, 143 (2007).
- [21] R. H. Hadfield, Single-photon detectors for optical quantum information applications, *Nat. Photon.* **3**, 696 (2009).
- [22] J.-L. Blanchet, F. Devaux, L. Furfaro, and E. Lantz, Measurement of Sub-Shot-Noise Correlations of Spatial Fluctuations in the Photon-Counting Regime, *Phys. Rev. Lett.* **101**, 233604 (2008).
- [23] P.-A. Moreau, J. Mougín-Sisini, F. Devaux, and E. Lantz, Realization of the purely spatial Einstein-Podolsky-Rosen paradox in full-field images of spontaneous parametric down-conversion, *Phys. Rev. A* **86**, 010101(R) (2012).
- [24] V. Chille, N. Treps, C. Fabre, G. Leuchs, C. Marquardt, and A. Aiello, Detecting the spatial quantum uncertainty of bosonic systems, *New J. Phys.* **18**, 093004 (2016).
- [25] A. E. Lita, A. J. Miller, and S. W. Nam, Counting near-infrared single-photons with 95% efficiency, *Opt. Express* **16**, 3032 (2008).
- [26] G. Brida, L. Ciavarella, I. P. Degiovanni, M. Genovese, L. Lolli, M. G. Mingolla, F. Piacentini, M. Rajteri, E. Taralli, and M. G. A. Paris, Quantum characterization of superconducting photon counters, *New J. Phys.* **14**, 085001 (2012).
- [27] J. J. Renema, G. Frucci, Z. Zhou, F. Mattioli, A. Gaggero, R. Leoni, M. J. A. de Dood, A. Fiore, and M. P. van Exter, Modified detector tomography technique applied to a superconducting multiphoton nanodetector, *Opt. Express* **20**, 2806 (2012).
- [28] H. Paul, P. Törmä, T. Kiss, and I. Jex, Photon Chopping: New Way to Measure the Quantum State of Light, *Phys. Rev. Lett.* **76**, 2464 (1996).

- [29] P. Kok and S. L. Braunstein, Detection devices in entanglement-based optical state preparation, *Phys. Rev. A* **63**, 033812 (2001).
- [30] D. Achilles, C. Silberhorn, C. Śliwa, K. Banaszek, and I. A. Walmsley, Fiber-assisted detection with photon number resolution, *Opt. Lett.* **28**, 2387 (2003).
- [31] M. J. Fitch, B. C. Jacobs, T. B. Pittman, and J. D. Franston, Photon-number resolution using time-multiplexed single-photon detectors, *Phys. Rev. A* **68**, 043814 (2003).
- [32] S. A. Castelletto, I. P. Degiovanni, V. Schettini, and A. L. Migdall, Reduced deadtime and higher rate photon-counting detection using a multiplexed detector array, *J. Mod. Opt.* **54**, 337 (2007).
- [33] V. Schettini, S.V. Polyakov, I.P. Degiovanni, G. Brida, S. Castelletto, and A.L. Migdall, Implementing a Multiplexed System of Detectors for Higher Photon Counting Rates, *IEEE J. Sel. Top. Quantum Electron.* **13**, 978 (2007).
- [34] J. Sperling, W. Vogel, and G. S. Agarwal, Sub-Binomial Light, *Phys. Rev. Lett.* **109**, 093601 (2012).
- [35] T. J. Bartley, G. Donati, X.-M. Jin, A. Datta, M. Barbieri, and I. A. Walmsley, Direct Observation of Sub-Binomial Light, *Phys. Rev. Lett.* **110**, 173602 (2013).
- [36] J. Sperling, M. Bohmann, W. Vogel, G. Harder, B. Brecht, V. Ansari, and C. Silberhorn, Uncovering Quantum Correlations with Time-Multiplexed Click Detection, *Phys. Rev. Lett.* **115**, 023601 (2015).
- [37] R. Heilmann, J. Sperling, A. Perez-Leija, M. Gräfe, M. Heinrich, S. Nolte, W. Vogel, and A. Szameit, Harnessing click detectors for the genuine characterization of light states, *Sci. Rep.* **6**, 19489 (2016).
- [38] J. Sperling, T. J. Bartley, G. Donati, M. Barbieri, X.-M. Jin, A. Datta, W. Vogel, and I. A. Walmsley, Quantum Correlations from the Conditional Statistics of Incomplete Data, *Phys. Rev. Lett.* **117**, 083601 (2016).
- [39] G. Harder, T. J. Bartley, A. E. Lita, S. W. Nam, T. Gerrits, and C. Silberhorn, Single-Mode Parametric-Down-Conversion States with 50 Photons as a Source for Mesoscopic Quantum Optics, *Phys. Rev. Lett.* **116**, 143601 (2016).
- [40] U. M. Titulaer and R. J. Glauber, Correlation functions for coherent fields, *Phys. Rev.* **140**, B676 (1965).
- [41] L. Mandel, Non-classical states of the electromagnetic field, *Phys. Scr.* **T12**, 34 (1986).
- [42] J. Sperling, *et al.*, Identification of nonclassical properties of light with multiplexing layouts, [arXiv:1701.07642 \[quant-ph\]](https://arxiv.org/abs/1701.07642).
- [43] The notion of a bin is used here synonymous with measurement outcome. It should not be confused with the concept of a temporal bin, which is used to describe time-bin multiplexing detectors [30, 31].
- [44] See C. Forbes, M. Evans, N. Hastings, and B. Peacock, *Statistical Distributions*, 4th ed. (Wiley & Sons, Hoboken, New Jersey, USA, 2011), Chap. 30.
- [45] See Supplemental Material, which includes Refs. [36, 42], for the error analysis and an additional study of the non-linear detector response of the TESs.
- [46] J. Sperling, W. Vogel, and G. S. Agarwal, True photocounting statistics of multiple on-off detectors, *Phys. Rev. A* **85**, 023820 (2012).
- [47] A. Eckstein, A. Christ, P. J. Mosley, and C. Silberhorn, Highly Efficient Single-Pass Source of Pulsed Single-Mode Twin Beams of Light, *Phys. Rev. Lett.* **106**, 013603 (2011).
- [48] K. D. Irwin, An application of electrothermal feedback for high resolution cryogenic particle detection, *Appl. Phys. Lett.* **66**, 1998 (1995).
- [49] P. C. Humphreys, B. J. Metcalf, T. Gerrits, T. Hiemstra, A. E. Lita, J. Nunn, S. W. Nam, A. Datta, W. S. Kolthammer, and I. A. Walmsley, Tomography of photon-number resolving continuous-output detectors, *New J. Phys.* **17**, 103044 (2015).
- [50] T. Gerrits, *et al.*, On-chip, photon-number-resolving, telecommunication-band detectors for scalable photonic information processing, *Phys. Rev. A* **84**, 060301(R) (2011).
- [51] See an analysis in G. S. Agarwal, *Quantum Optics* (Cambridge University Press, Cambridge, 2013), including Fig. 3.2.
- [52] G. S. Agarwal and K. Tara, Nonclassical character of states exhibiting no squeezing or sub-Poissonian statistics, *Phys. Rev. A* **46**, 485 (1992).
- [53] I. I. Arkhipov, J. Peřina, O. Haderka, and V. Michálek, Experimental detection of nonclassicality of single-mode fields via intensity moments, *Opt. Express* **24**, 29496 (2016).

Supplemental Material: Detector-Independent Verification of Quantum Light

J. Sperling,¹ W. R. Clements,¹ A. Eckstein,¹ M. Moore,¹ J. J. Renema,¹ W. S. Kolthammer,¹
S. W. Nam,² A. Lita,² T. Gerrits,² W. Vogel,³ G. S. Agarwal,⁴ and I. A. Walmsley¹

¹*Clarendon Laboratory, University of Oxford, Parks Road, Oxford OX1 3PU, United Kingdom*

²*National Institute of Standards and Technology, 325 Broadway, Boulder, CO 80305, USA*

³*Institut für Physik, Universität Rostock, Albert-Einstein-Straße 23, D-18059 Rostock, Germany*

⁴*Texas A&M University, College Station, Texas 77845, USA*

(Dated: March 20, 2017)

This supplemental material is organized as follows. In part **A**, we present the essential details of our data processing and error analysis. In part **B**, the detector response of a single detector is analyzed. The used acronyms are TES (transition-edge sensor) and PDC (parametric down-conversion).

Appendix A: Data processing and error analysis

For the application of our approach, we provide the data-analysis methods. With the detection scheme under study, employing N detectors which resolve $K + 1$ outcomes, one measures the coincidence counts $C_{\vec{k}}$, with $\vec{k} = (k_1, \dots, k_N) \in \{0, \dots, K\}^N$ labeling the event that the n th detector yields the measurement outcome k_n . The total number of counts is given by $C = \sum_{\vec{k}} C_{\vec{k}} = \|C_{\vec{k}}\|$. Our numerical data analysis is implemented as described here and in terms of such arrays $C_{\vec{k}}$. Therefore, we use this multi-index notation to ensure reproducibility.

From individual counts $C_{\vec{k}}$ to the click counting statistics $c(N_0, \dots, N_K)$. The numbers N_k —number of detectors that give the outcome k —can be also arranged in the $(K + 1)$ -dimensional multi-index $\vec{N} = (N_0, \dots, N_K)$. For our multiplexing scheme, the relation to \vec{k} is given by the summation

$$\vec{N} = \nu(\vec{k}) \stackrel{\text{def.}}{=} \sum_n \vec{e}_{k_n}, \quad (\text{A1})$$

where $\vec{e}_k = (\delta_{k,l})_{l=0, \dots, K}$ is the k th standard basis vector. Note that $\|\vec{N}\| = \sum_k N_k = N$. Then, the click-counting statistics can be directly written as

$$c(N_0, \dots, N_K) = c(\vec{N}) = \frac{1}{C} \sum_{\vec{k}: \nu(\vec{k}) = \vec{N}} C_{\vec{k}}. \quad (\text{A2})$$

In our case of $N = 2$ detectors, we measured the raw counts $C_{(k_1, k_2)}$ with two TESs, and the total number of counts is $C = \sum_{k_1, k_2=0}^K C_{k_1, k_2}$. For the only possible cases of indices with $\|\vec{N}\| = N = 2$, we get the click counting statistics from Eq. (A2) as

$$c(\vec{N}) = \frac{1}{C} \begin{cases} C_{k,k} & \text{for } \vec{N} = 2\vec{e}_k, \\ C_{k,k'} + C_{k',k} & \text{for } \vec{N} = \vec{e}_k + \vec{e}_{k'}, \end{cases} \quad (\text{A3})$$

where the first case corresponds to a measurement of k from both detectors and the second case is that both detectors give different outcomes $k \neq k'$.

Systematic error from asymmetric data. For a balanced multiplexing and identical detectors, all permutations $P_\tau \vec{k}$ of elements of \vec{k} give the same count rates, $C_{P_\tau \vec{k}} = C_{\vec{k}}$, where P_τ is the operator which redistributes the components of \vec{k} according to the permutation $\tau \in \mathcal{S}_N$. Hence, the deviation from this symmetry results in a relative systematic error,

$$\varepsilon_{\text{sys}} = \sum_{\tau \in \mathcal{S}_N} \frac{\|C_{\vec{k}} - C_{P_\tau \vec{k}}\|}{C}. \quad (\text{A4})$$

In combination with a relative statistical error $\varepsilon_{\text{stat}}$ for the estimate \bar{f} of a quantity f , we have $f = \bar{f}(1 \pm [\varepsilon_{\text{stat}} + \varepsilon_{\text{sys}}]) = \bar{f} \pm \Delta f$. For two TESs, Eq. (A4) simplifies to

$$\varepsilon_{\text{sys}} = \frac{1}{C} \sum_{k, k'=0}^K |C_{k, k'} - C_{k', k}|. \quad (\text{A5})$$

Sampling of moments. In order to sample a quantity f , which is a function of the number of coincidences \vec{N} , we obtain from Eqs. (A1) and (A2)

$$\bar{f} = \sum_{\vec{N}} f(\vec{N}) c(\vec{N}) = \frac{1}{C} \sum_{\vec{k}} f(\nu(\vec{k})) C_{\vec{k}}, \quad (\text{A6})$$

where we applied $\sum_{\vec{N}} \sum_{\vec{k}: \nu(\vec{k}) = \vec{N}} = \sum_{\vec{k}}$. The standard error of the mean reads $\sigma(\bar{f}) = [(\bar{f}^2 - \bar{f}^2)/(C - 1)]^{1/2}$, which gives the relative statistical error $\varepsilon_{\text{stat}} = \sigma(\bar{f})/|\bar{f}|$. For example, we can use $f(\vec{N}) = \vec{N}^{\vec{w}} = \prod_k N_k^{w_k}$ to get for the moments:

$$f(\vec{N}) = \prod_k \left(\sum_n \delta_{k, k_n} \right)^{w_k} \quad (\text{A7})$$

using $N_k = \vec{e}_k \cdot \nu(\vec{k}) = \sum_n \delta_{k, k_n}$ [cf. Eq. (A1)] and $\vec{e}_k \cdot \vec{e}_{k'} = \delta_{k, k'}$.

For the example of the first-order moments (mean values) and two TESs, Eqs. (A6) and (A7) explicitly give

$$\bar{N}_k = \frac{1}{C} \left[\sum_{k_1=0}^K C_{k_1, k} + \sum_{k_2=0}^K C_{k, k_2} \right], \quad (\text{A8})$$

for $k = 0, \dots, K$. Analogously, the second-order moments read

$$\overline{N_k N_{k'}} = \frac{1}{C} \left[C_{k,k'} + C_{k',k} + \delta_{k,k'} \left(\sum_{k_1=0}^K C_{k_1,k} + \sum_{k_2=0}^K C_{k,k_2} \right) \right]. \quad (\text{A9})$$

Error propagation. For the propagation of errors, a linear error propagation is favorable as the systematic error might exceed the statistical error. From the sampled moments, we get the elements of the matrix M , used in the Letter, and their errors. For this matrix $M = \overline{M} \pm \Delta M$ and a given vector \vec{f} , the linear error propagation yields

$$\mu = \vec{f}^\dagger M \vec{f} = \vec{f}^\dagger \overline{M} \vec{f} \pm |\vec{f}^\dagger \Delta M \vec{f}|, \quad (\text{A10})$$

where $|\cdot|$ acts component-wise on the vector \vec{f} .

Suppose \vec{f} is a normalized eigenvector to the matrix \overline{M} , i.e., $\overline{M} \vec{f} = \overline{\mu} \vec{f}$ and $\vec{f}^\dagger \vec{f} = 1$. Then the eigenvalue μ of M is represented via the mean value $\overline{\mu} = \vec{f}^\dagger \overline{M} \vec{f}$. From Eq. (A10), we also get its error $\Delta\mu = |\vec{f}^\dagger \Delta M \vec{f}|$. See Ref. [1] for further details.

Appendix B: Detector response

Our detector-independent approach does not require to know specific detector characteristics for the verification of nonclassicality. However, since the TESs used are at the cutting edge of detector technology, we provide an additional discussion on the detector response. This also demonstrates the complex behavior of our detectors and the necessity to formulate detector-independent nonclassicality tests.

Reference states. To identify properties of the TES, we measured one mode of the two-mode squeezed-vacuum state, which is produced by our PDC source, with a single TES. It is well known that the marginal photon-number distribution $p(n)$ of this state is given by a geometric distribution,

$$p(n) = (1 - \lambda)\lambda^n, \quad (\text{B1})$$

where $0 < \lambda < 1$. In Fig. 1, the measurement outcome is shown [see also Fig. 2(b) in the Letter].

Reference measurement. We can see in Fig. 1 that we can resolve 11 peaks (indicated by bullets and vertical dark green, solid lines). They correspond to the discrete energy levels E_n of the n -photon contribution. The difference between two discrete energies E_n is not constant as one would expect from $E_n = \hbar\omega n + E_0$. Also, the marginal photon statistics is the geometric distribution (B1) which, in the logarithmic scaling in Fig. 1, would result in the linear function $\log_{10} p(n) = n \log_{10} \lambda + \log_{10}(1 - \lambda)$. However, we observe a deviation from such a model; compare light green, dashed and dot-dashed lines in Fig. 1.

Nonlinear response. Rather than a linear function, the quadratic fit of the peaks in Fig. 1 properly describes our data. This shows that the TES, together with the employed superconducting quantum interference device (SQUID) module, has a nonlinear response to the energy of the incident photons. In particular, this also implies that the measured statistics for different λ values is more complex than the geometric form of marginal photon statistics (B1); see also [2] for further details.

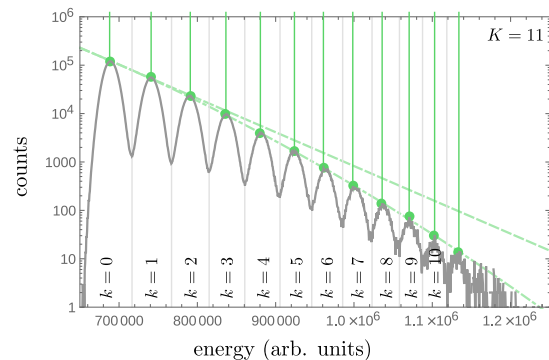


FIG. 1. The counts of one TES (solid, gray curve) are depicted. Maxima for all $k \in \{0, \dots, K\}$ bins are shown as bullets. The green vertical lines correspond to the energy levels of the maxima. A nonlinear regression ($\log_{10} y = ax^2 + bx + c$; green, dot-dashed line) and its tangent at the first maximum (green, dashed line) are additionally shown.

[1] J. Sperling, M. Bohmann, W. Vogel, G. Harder, B. Brecht, V. Ansari, and C. Silberhorn, Uncovering Quantum Correlations with Time-Multiplexed Click Detection, *Phys. Rev. Lett.* **115**, 023601 (2015).

[2] J. Sperling, A. Eckstein, W. R. Clements, M. Moore, J. J. Renema, W. S. Kolthammer, S. W. Nam, A. Lita, T. Gerrits, I. A. Walmsley, G. S. Agarwal, and W. Vogel, Identification of nonclassical properties of light with multiplexing layouts, [arXiv:1701.07642](https://arxiv.org/abs/1701.07642) [quant-ph].